*Radio Science*, Volume 30, Number 6, Pages 1699–1712, November–December 1995

# Analysis of electromagnetic wave direction finding performed by spaceborne antennas using singular-value decomposition techniques

H. P. Ladreiter,[1] P. Zarka,[2] A. Lecacheux,[2] W. Macher,[1] H. O. Rucker,[1] R. Manning,[2] D. A. Gurnett,[3] and W. S. Kurth [3]

**Abstract.** By using two rotating noncollinear antennas or three spatially fixed noncoplanar antennas on a spacecraft, full information on the polarization and the direction of arrival of an electromagnetic wave can be obtained by measuring the voltages created by the electric field of the incident wave. The physical parameters (polarization and direction of arrival) of the incoming wave are related to the received voltages on the antenna system by the so-called direction-finding equations. Since the used antennas are generally of small directivity (electrically short monopoles or dipoles), the resulting system of equations is numerically close to singular, and generally no unique solution can be obtained for the physical parameters of the wave throughout the inversion process. However, there exists a very powerful tool for dealing with sets of equations that are singular or close to singular, known as singular-value decomposition (SVD), which precisely focuses the problem. For illustration, this paper analyzes the direction-finding equations for the Radio and Plasma Wave Science (RPWS) experiment on the Cassini spacecraft by using SVD techniques. It also compares the expected performances of RPWS with those of the Ulysses Unified Radio and Plasma Wave (URAP) experiment achieved at Jupiter for the kilometer and hectometer emissions. The RPWS experiment on Cassini, which will be launched in 1997, is supposed to observe wave phenomena between a few hundred Hertz and 16 MHz in the Saturnian magnetosphere.

## 1. Introduction

Direction finding (i.e., determination of the radio emission's source direction and of the full polarization of the wave) from measured voltages received by the electrical antennas) is an important task of the Radio and Plasma Wave Science (RPWS) experiment on Cassini. The technique has demonstrated its usefulness at Jupiter where it allowed location and measurement of the polarization of all nonthermal Jovian radio components in the kilometer-to-hectometer range [*Reiner et al.*, 1993a; *Ladreiter et al.*, 1994] using data of the Unified Radio and Plasma Wave (URAP) experiment [*Stone et al.*, 1992] on board the Ulysses spacecraft.

The RPWS electric antenna system on the Cassini spacecraft is a system of three conducting monopoles (each of them 10 m long), symmetrical about the $y$-$z$ plane, as shown in Figure 1. Two of the elements (X, -X) are extended in a 120° "V" on either side of the magnetometer boom along the $y$-axis. The +X,-X-plane is inclined by 37° relative to the $x$-$y$-plane. The

[1]Space Research Institute, Austrian Academy of Sciences, Graz, Austria.

[2]Observatoire de Paris, Meudon, France.

[3]Department of Physics and Astronomy, University of Iowa, Iowa City.



Paper number 95RS02479.
0048-6604/95/95RS-02479$08.00

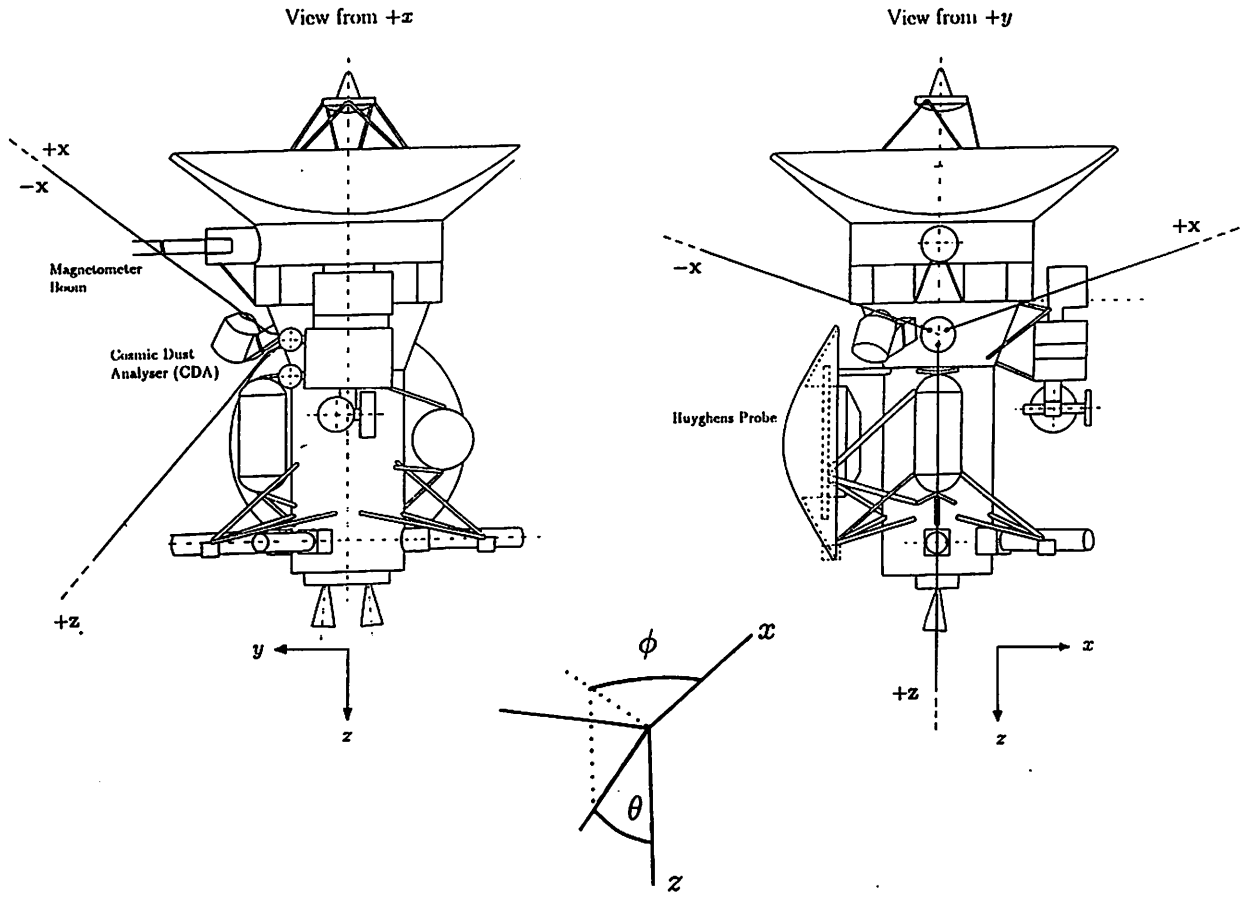


**Figure 1.** RPWS antenna system on the Cassini spacecraft and associated coordinate system used throughout this work. The angles $\theta = 90° - \arctan(z/\sqrt{x^2+y^2})$ (colatitude) and $\phi = \arctan(y/x)$ (azimuth) refer to a spherical coordinate system based on the cartesian axes $x$, $y$, $z$ as shown (adapted from H. O. Rucker et al., submission, 1995).

third element (Z) is extended downward in the $y$-$z$ plane at an angle of 37° from the $z$-axis of the spacecraft (i.e., perpendicular to the +X,-X-plane). While these three antennas can be utilized in many ways by the RPWS instrument, the mode of interest here is their use as a triaxial antenna system for direction-finding.

At Saturn this system will be used to study the Saturnian kilometric radiation (SKR) and the so-called Saturn electrostatic discharges (SED) (actually lightning radio emission) [*Kaiser et al.*, 1984; *Boischot*, 1988; *Zarka*, 1985]. The required precision in the radio source direction allowing identification of the active L-shell (for SKR) or storm system (for SED) is a small fraction of 1 Saturnian radius ($R_S$), or about 1° from a typical 10 $R_S$ range. Consequently, an "a priori" estimate of the instrument's performance allows us to anticipate the precision of direction-finding in terms of source location and wave polarization.

In section 2 of this report we therefore discuss the direction-finding theory as it applies to the RPWS experiment. We show that singular-value decomposition (SVD) techniques provide a straightforward way to obtain information on how well the required wave parameters (polarization and direction of arrival) are determined by the direction-finding equations. We perform a singular-value analysis of the RPWS direc-

tion-finding equations and recognize that if the direction-finding equations are ill-conditioned, no unique solution can be found for the wave parameters, and, consequently, linear dependence between wave parameters occurs. In this respect, the Cassini RPWS experiment is compared and contrasted to the Unified Radio and Plasma Wave (URAP) experiment [*Stone et al.*, 1992] on the Ulysses spacecraft that enabled the investigation (by performing direction-finding) of the Jovian nonthermal radio emissions below 1 MHz in February 1992. In the last part of this paper we estimate the precision of RPWS direction-finding (e.g., for the Saturnian emissions) as a function of the statistical uncertainty of the observations.

## 2. Direction-Finding Analysis

We first derive the relevant equations which associate the modeled quantities $< V_n V_k^* >^{\mathrm{mod}}$ to the electric field $\mathbf{E}$ of the incident wave. The $< V_n V_k^* >^{\mathrm{obs}}$ are the corresponding data to be measured by the RPWS experiment. $V_n$ denotes the voltage received on antenna $n$, the asterisk denotes the complex conjugate, and $<\ >$ is the time-averaging operation.

$$< V_n V_k^* >^{\mathrm{mod}} = < (\mathbf{h}_n \mathbf{E})(\mathbf{h}_k \mathbf{E})^* > \qquad (1)$$

where $\mathbf{h}_n$ is the effective height of antenna $n$. To compute (1), $\mathbf{h}_n$, $\mathbf{h}_k$, and $\mathbf{E}$ must refer to a common coordinate system $(O, X_w, Y_w, Z_w)$, as shown in Figure 2. In the study of the polarization response of our antenna system (Figure 1), the effective height $\mathbf{h}_n(\theta_n, \phi_n)$ must therefore be expressed in the same reference frame as the wave polarization components. Let us construct this wave coordinate system $(O, X_w, Y_w, Z_w)$ by by taking $OX_w$ as being the projection of the $oz$ direction of the plane wave, as shown in Figure 2; $OX_w$ will be our reference for defining the state of polarization. $OZ_w$ is taken to be parallel to the wave vector $\mathbf{k}$. $OY_w$ completes the right-hand coordinate system.

Figure 2 relates the antenna coordinate system $(o, x, y, z)$ used in Figure 1 to the wave system $(O, X_w, Y_w, Z_w)$. From Figure 2 we see that the components of the effective height $\mathbf{h}_n$ of antenna $n$ in the wave coordinate system $(O, X_w, Y_w, Z_w)$ are defined by

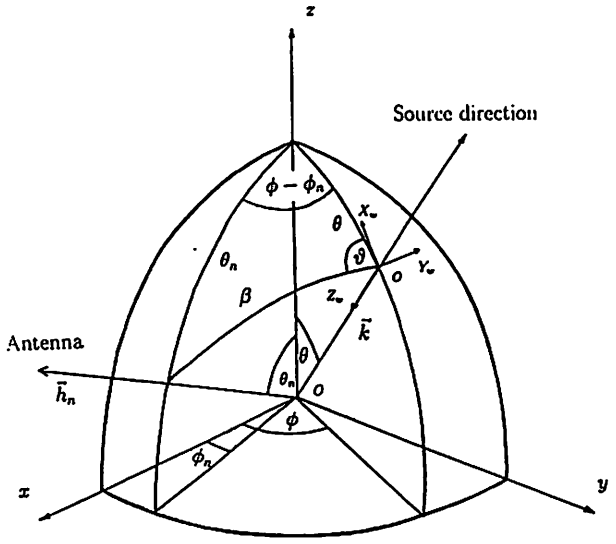


**Figure 2.** Coordinate systems used for derivation of the modeled antenna signals throughout the text showing the antenna system $(o, x, y, z)$ and the wave system $(O, X_w, Y_w, Z_w)$. Here $\theta_n$ and $\phi_n$ define the effective height direction of antenna $n$. $\theta$ and $\phi$ are the source direction angles, as shown.

$$\begin{aligned} h_{n,Xw} &= h_n \sin\beta \cos\vartheta \\ h_{n,Yw} &= h_n \sin\beta \sin\vartheta \end{aligned} \qquad (2)$$

where $h_n$ is the modulus of $\mathbf{h}_n$. Using the relations

$$\begin{aligned} \cos\beta &= \cos\theta_n \cos\theta + \sin\theta_n \sin\theta \cos(\phi - \phi_n) \\ \cos\theta_n &= \cos\beta \cos\theta + \sin\beta \sin\theta \cos\vartheta \end{aligned}$$

we end up with

$$\begin{aligned} h_{n,Xw} &= h_n[\cos\theta_n \sin\theta - \\ &\qquad \sin\theta_n \cos\theta \cos(\phi - \phi_n)] \\ h_{n,Yw} &= -h_n \sin\theta_n \sin(\phi - \phi_n). \end{aligned} \qquad (3)$$

Thus we derived the components of $\mathbf{h}_n$ in the wave system $(O, X_w, Y_w, Z_w)$ as a function of $\theta_n$

(denoting the colatitude of $\mathbf{h}_n$ with respect to the $z$-axis), $\theta$ (colatitude of the source), and $\phi - \phi_n$ (azimuth of the source minus the azimuth of $\mathbf{h}_n$).

To characterize the electric field of the incoming plane wave we can write

$$\begin{aligned} E_{Xw} &= a_1 e^{i\omega t} \\ E_{Yw} &= a_2 e^{i(\omega t - \delta)} \end{aligned} \tag{4}$$

where $\omega$ is the angular frequency of the wave and $\delta$ is the phase shift between the $E_{Xw}$ and $E_{Yw}$ components. The $Z_w$ component of $\mathbf{E}$ is zero since the plane containing $\mathbf{E}$ is perpendicular to the wave normal direction $Z_w$. We chose the indices $X_w$ and $Y_w$ to emphasize that $\mathbf{E}$ refers to the wave system $(O, X_w, Y_w, Z_w)$. The amplitude and state of polarization of the incoming wave are completely defined by (4). Combining (3) and (4) we find

$$\begin{aligned} V_n = h_n(a_1 e^{i\omega t}[&\cos\theta_n \sin\theta \\ &- \sin\theta_n \cos\theta \cos(\phi - \phi_n)] \\ &- a_2 e^{i(\omega t - \delta)} \sin\theta_n \sin(\phi - \phi_n)) \end{aligned} \tag{5}$$

Squaring (5) and time averaging over $T >> 2\pi/\omega$ yields the required quantities

$$\begin{aligned} Re < V_n V_k^* >^{\mathrm{mod}} = \frac{S h_n h_k}{2}((1+Q)\Omega_n \Omega_k \\ -U(\sin\theta_k \sin(\phi - \phi_k)\Omega_n - \sin\theta_n \sin(\phi - \phi_n)\Omega_k) \\ +(1-Q)\sin\theta_n \sin\theta_k \sin(\phi - \phi_n)\sin(\phi - \phi_k)) \end{aligned} \tag{6}$$

$$\begin{aligned} < Im < V_n V_k^* >^{\mathrm{mod}} = \\ \frac{S h_n h_k}{2} V(\sin\theta_k \sin(\phi - \phi_k)\Omega_n \\ - \sin\theta_n \sin(\phi - \phi_n)\Omega_k) \end{aligned} \tag{7}$$

where $\Omega_n = \cos\theta_n \sin\theta - \sin\theta_n \cos\theta \cos(\phi - \phi_n)$, and $h_n$, $\theta_n$, and $\phi_n$ are the spherical coordinates of the effective height $\mathbf{h}_n$ of antenna $n$, as shown in Figures 1 and 2.

The Stokes parameters $S, Q, U, V$ are defined by [*Kraus*, 1966]

$$\begin{aligned} S &= < a_1^2 + a_2^2 > /2 \\ Q &= \frac{< a_1^2 - a_2^2 >}{S} \\ U &= \frac{2 < a_1 a_2 \cos\delta >}{S} \\ V &= \frac{2 < a_1 a_2 \sin\delta >}{S} \end{aligned} \tag{8}$$

$S$ is $Z$-times the modulus of the Poynting vector where $Z$ is the antenna impedance. Equations (6) and (7) can also be derived in terms of the coherency matrix formalism followed by *Lecacheux* [1978].

Once we have found the modeled expressions $< V_n V_k^* >^{\mathrm{mod}}$ in terms of the source direction and Stokes parameters via (6) and (7), we are free to find methodologies to derive the wave parameters $\mathbf{X} = (S, Q, U, V, \theta, \phi)$ from the $< V_n V_k >^{\mathrm{mod}}$ by setting $< V_n V_k >^{\mathrm{mod}}$ equal to the measured $< V_n V_k >^{\mathrm{obs}}$ as observed by the RPWS experiment. An index $j$ can be used to denote the components of $\mathbf{X}$ (e.g., $X_{j=1} = S$, $X_{j=4} = V$). A so-called closed form solution obtained by calculating $\mathbf{X}$ directly from (6) and (7), as well as a least squares solution obtained by requiring that the sum of the modeled minus observed quantities squared should be a minimum, have been elaborated by *Manning and Fainberg* [1980]. In this paper we use a more general technique, based on the least squares requirement, that in addition allows checking whether unique solutions $\mathbf{X}$ can be obtained throughout the inversion process.

In order to find the model parameter vector $\mathbf{X}$ that contains the unknown wave parameters we search for a solution where the weighted least squared sum of the differences between the RPWS-observations $y_i^{\mathrm{obs}}$ and the model-predicted values $y_i^{\mathrm{mod}}$ becomes a minimum:

$$\chi^2 = \sum_{i=1}^{N} W_i \, (y_i^{\mathrm{obs}} - y_i^{\mathrm{mod}}(\mathbf{X}))^2 = \mathrm{Min} \tag{9}$$

The $y_i^{obs}$ represent the squared voltages $< V_1V_1^* >$, $< V_2V_2^* >$, $< V_3V_3^* >$, $Re < V_1V_3^* >$, $Re < V_2V_3^* >$, $Im < V_1V_3^* >$, and $Im < V_2V_3^* >$ provided by the RPWS measurements. The index 1 refers to the X-antenna, 2 to the -X-antenna, and 3 to the Z-antenna (Figure 1). The $y_i^{mod}$ represents the theoretical expressions of the measured signals $< V_nV_k^* >^{mod} = < (\mathbf{h}_n\mathbf{E})(\mathbf{h}_k\mathbf{E})^* >$ as defined by (6) and (7).

The $W_i$ are the weights reflecting the uncertainty of each $y_i^{obs}$. The $W_i$ are in general proportional to $(y_i^{obs})^{-2}$ defined by the automatic gain control (AGC) value of the observation $i$ to account for the constant relative error in the data. The vector $\mathbf{X}$ contains the wave parameters to be determined (i.e., $\mathbf{X} = (S, Q, U, V, \theta, \phi)$) for direction-finding. To find the solution for (9) we perform differentiation with respect to the components $X_j$ of the vector $\mathbf{X}$:

$$\frac{\partial \chi^2}{\partial X_j} = 0 \tag{10}$$

It can be easily seen from (6) and (7) that $\chi^2$ is not linear with regard to the components $X_j$ after differentiation, thus linearization is required:

$$\frac{\partial \chi^2}{\partial X_j}\Big|_{\mathbf{X}^o} = -\frac{\partial^2 \chi^2}{\partial X_j \partial X_k}\Big|_{\mathbf{X}^o} \cdot \Delta X_k \tag{11}$$

The term $\partial^2\chi^2/(\partial X_j \partial X_k)$ represents a six-times-six symmetrical square matrix containing the partial derivatives of $\chi^2$ with respect to $X_j$ and $X_k$. The matrix element $j = 5$, $k = 6$, for example, denotes $\partial^2\chi^2/(\partial\theta\partial\phi)$. Rapid convergence of the iteration process is ensured if (11) denotes a well-posed system of equations. Iteration should be performed until $\Delta X_k$ is small. A good initial guess $\mathbf{X}^o$ (not too far from $\mathbf{X}$ that minimizes $\chi^2$) is necessary for ensuring rapid convergence of the process.

Equation (11) can be written in the form

$$b_j = A_{jk}\,\Delta X_k \tag{12}$$

Since the iteration procedure may be not efficient for ill-posed systems of equations we apply singular-value decomposition (SVD) (see appendix) to see whether or not the matrix $A$ is basically of full rank:

$$\mathbf{b} = U\,\Lambda\,V^T\Delta\mathbf{X} \tag{13}$$

where the matrices $V$ and $U$ are coloumnwise composed of the eigenvectors of $A^TA$ and $AA^T$, respectively. Here $U = V$ since $A$ is symmetrical (the superscript $T$ denotes the transpose of a matrix). $\Lambda$ is a diagonal matrix containing the singular values of $A$:

$$\Lambda = \begin{pmatrix} \lambda_1 & 0 & \dots & \dots \\ 0 & \lambda_2 & \dots & \dots \\ \vdots & \vdots & \ddots & \dots \\ \vdots & \vdots & \vdots & \lambda_n \end{pmatrix}$$

The singular values $\lambda_i$ of $A$ correspond to the squareroot of eigenvalues of the matrix $AA^T$ or $A^TA$.

Inverting (13) we finally obtain the system of linearized direction-finding equations that was previously solved by iteration (see also *Press et al.* [1986] and references therein):

$$\Delta\mathbf{X} = V\,\Lambda^{-1}\,U^T\,\mathbf{b} \tag{14}$$

where $V\Lambda^{-1}U^T = A^+$ is called the generalized inverse of $A$, and $\Lambda^{-1}$ is the inverse of $\Lambda$ containing the inverse of the $\lambda_n$:

$$\Lambda^{-1} = \begin{pmatrix} 1/\lambda_1 & 0 & \dots & \dots \\ 0 & 1/\lambda_2 & \dots & \dots \\ \vdots & \vdots & \ddots & \dots \\ \vdots & \vdots & \vdots & 1/\lambda_n \end{pmatrix}$$

Special insight into the equation system can be obtained by inspection of $\Lambda$. If the variances of the components $X_j$ are of similar size, the effective number of linear independent equations can be identified by counting the number of significant singular values, excluding those whose value is 0 or practically 0. If the number of significant singular values is equal to the number of unknowns in $\mathbf{X}$ (six in our case), then the components $X_j$ of $\mathbf{X}$ are well-defined by the system of equations. If the number of signifi-

cant singular values is less than the number of unknowns, then the solution vector $\mathbf{X}$ has no unique solution and the system of equations is ill-conditioned. In constructing our solution vector $\mathbf{X}$ obtained by iteration using $\Delta\mathbf{X}$ from (14), we are then free to eliminate the near-zero singular values (and the corresponding eigenvectors), reducing the parameter variance to a lower level by simultaneously keeping $\chi^2$ statistically at its minimum value as required by (9). By this technique we avoid, at the expense of a loss of model parameter resolution, a large contribution of poorly defined parameters due to a small noise component on the data. Parameter resolution is described by the resolution matrix $R$ (see *Connerney* [1981] and references therein) relating the solution $\mathbf{X}(l)$ using $l$ eigenvectors to the solution $\mathbf{X}$ using all eigenvectors (including those associated with small singular values) that represents the traditional least squares solution.

$$\mathbf{X}(l) = R(l)\mathbf{X} \tag{15}$$

where $R(l) = V(l)V(l)^T$ and the index $l$ to a matrix denotes the matrix obtained by setting each column $i$ for $i > l$ of the original matrix to zero. If no eigenvector is set to zero, then $R$ is the identity matrix; as fewer eigenvectors are admitted in the construction of the solution, the off-diagonal elements of the $R$ matrix grow at the expense of the diagonal elements, denoting a loss of parameter resolution. The off-diagonal elements of the resolution matrix $R$ describe linear combinations of parameters which are zero only if the number of equations in consideration is equal to the number of unknowns.

## 3. Results

### 3.1. Singular-Value Analysis of RPWS Direction-Finding Equations

We have stated in section 2 that the SVD analysis of the direction-finding equations yields the matrix $\Lambda$ containing the singular values of $A$. The ratio of the largest to the smallest singular value of that matrix, the condition number, is a relevant quantity that describes how well the system of equations (equation (14)) is determined to solve for the unknown parameter vector $\mathbf{X}$ that contains the wave parameters $S, Q, U, V, \theta, \phi$ when direction-finding is performed (for this statement, we tacitly assume that the variance for the components of $\mathbf{X}$ are comparable in magnitude). If the condition number is very large, say $10^4$, the system is ill-conditioned and the parameter vector $\mathbf{X}$ or at least some components of it are poorly determined. If it is low, say 10, then the parameters in $\mathbf{X}$ are well-defined and constrained by the respective equation system. In order to get information on the matrix $\Lambda$ for the RPWS experiment we have first to simulate the observations $y_i^{\text{obs}}$ and the $W_i$ in (9) by using (6) and (7). We take the Stokes parameters $Q = U = 0$, $V = -1$ as was typically observed for Saturnian kilometric radiation from the Voyager spacecraft [*Boischot*, 1988]. For simplicity we set $Sh_nh_k$ to unity (normalization) in (6) and (7) without loss of generality since the condition number of $\Lambda$ is not affected by this operation. The effective height directions are taken from rheometric measurements (H. O. Rucker et al., Cassini model rheometry, submitted to *Radio Science*, hereinafter referred to as submission, 1995) and are given in Table 1. A 3% random noise was added to the simulated data calculated from (6) and (7) to account for the quantization step uncertainty of the instrument during the analog-to-digital conversion. This procedure creates realistic da-

**Table 1.** Physical and Effective Height Directions of the RPWS-Antennas On Board the Cassini Spacecraft

| Antenna | h | | $h_{eff}$, HP On/HP Off | |
|---|---|---|---|---|
| | $\theta_n^p$ | $\phi_n^p$ | $\theta_n$ | $\phi_n$ |
| +x | 107.5 | 24.8 | 107.9/107.6 | 16.5/16.3 |
| -x | 107.5 | 155.2 | 107.3/106.4 | 162.7/163.5 |
| +z | 37.0 | 90.0 | 31.4/30.8 | 91.2/92.9 |

All angles are given in degrees and refer to the antenna coordinate system $(o, x, y, z)$ in Figure 1. The effective heights depend somewhat whether or not the Huygens probe (HP) is mounted, but this difference is not important for our study (from H. O. Rucker et al., submission, 1995).

ta sets for high signal-to-noise ratios. The $W_i$ are chosen accordingly.

With the simulated $y_i^{obs}$ as described, the condition number of the matrix $\Lambda$ is calculated from (13) as a function of the wave's direction of arrival (source direction), and we show the logarithm (basis 10) of the condition number for the RPWS experiment in Figure 3 (top). Excluding source locations near the polar regions ($\theta$ near 0° and 180°) and locations in the vicinity of the Z-antenna direction (defined in Table 1), the condition number is about 100 or less for a large range of source geometries. For comparison we plot the condition number for the Ulysses URAP experiment in Figure 3 (bottom). That condition number is also calculated from (14) and modified according to the Ulysses URAP characteristics [*Stone et al.*, 1992; *Reiner et al.*, 1993a; *Ladreiter et al.*, 1994]. The direction-finding measurements performed by the URAP experiment on Ulysses were based on a spinning antenna configuration (dipole and monopole) that collected 24 individual voltage measurements during one spin period (*Stone et al.*, 1992]. A total of 16 out of 24 measurements were of high enough quality to perform direction-finding of the Jovian kilometric and hectometric emissions [*Ladreiter et al.*, 1994]. Because the direction-finding analysis is based on a spinning geometry, the condition number is axisymmetric with respect to the spin axis (Z-axis); the slight azimuthal scattering on the data is only due to the 3% noise added to the basic model data. However, when comparing the top and bottom panels of Figure 3, we recognize that the condition number is generally lower for Cassini than for Ulysses for a wide range of source positions, thus the RPWS experiment is supposed to do wave parameter determination (direction-finding) as well as the URAP experiment. Since the error on the Ulysses URAP direction-finding is supposed to be less than some 2° in terms of source localization [*Ladreiter et al.*, 1994], we can be optimistic that the RPWS experiment is well suited to perform accurate direction-finding, too. Further evidence of this is outlined in section 3.3.

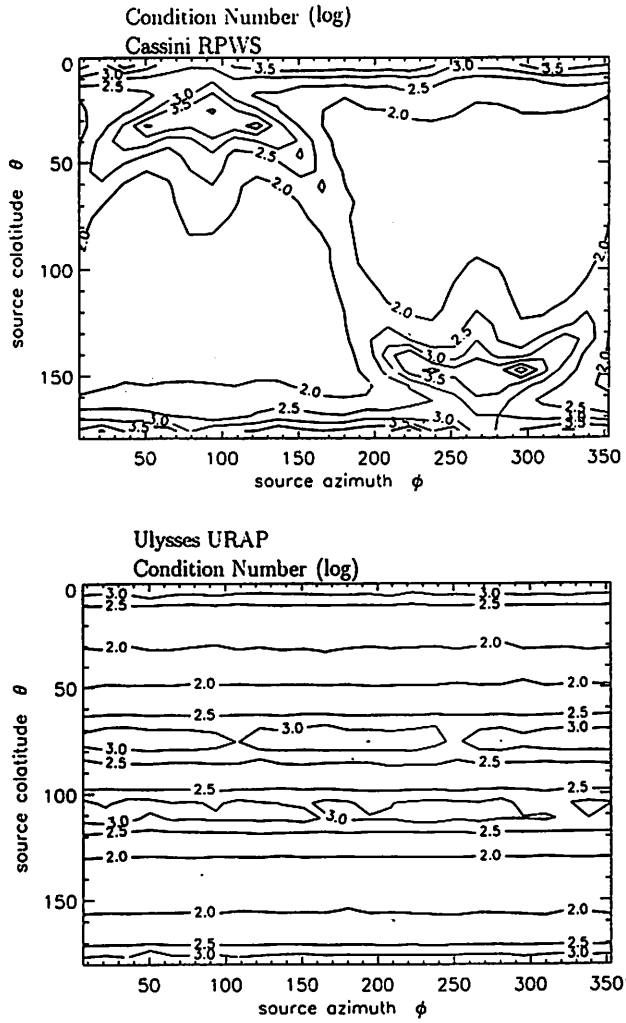


**Figure 3.** Logarithm of the condition number of the direction-finding equations (equation (14)) as a function of source position for (top) Cassini and (bottom) Ulysses. We notice that the condition number is generally somewhat lower for the Cassini RPWS than for the Ulysses URAP experiment.

The effective height directions are already determined by rheometric measurements; however, we can check these effective heights by calibration of the antenna system using a known (in terms of Stokes parameters and source direction) radio emission. This can be done when Cassini encounters the planet Jupiter during its journey to Saturn. The characteristics of the Jovian kilometric and hectometric radio emis-

sions in terms of source location and polarization are now well-known from the Ulysses URAP observations [*Reiner et al.*, 1993b; *Ladreiter et al.*, 1994]. To perform antenna calibration using the Jovian radio signals, we proceed as described in section 2, setting for the unknown parameter vector $\mathbf{X}=(S, \mathrm{h}_1, \mathrm{h}_2, \mathrm{h}_3)$ instead of $\mathbf{X}=(S, Q, U, V, \theta, \phi)$. The initial guess for the effective heights is given be the rheometric measurements as shown in Table 1.

### 3.2. Resolution and Linear Dependencies of the Wave Parameters

As we have shown in section 2, the condition number of the matrix $\Lambda$ is critical to the determination of the unknown parameter vector $\mathbf{X}$. If this ratio is high, the unknowns cannot be determined unambiguously from the system of equations (equation (14)) because the system contains fewer linear independent equations than unknowns. There exists no unique solution in parameter space $\mathbf{X}$ and consequently linear dependence between parameters occur that are associated with a loss of parameter resolution which are explicitly identified using SVD methodologies (equation (15)). The resolution matrix is distinct from the unity matrix when the number of statistically significant singular values (setting them to zero in (14) would produce a significant enhancement of $\chi^2$ defined by (9)) is lower than the number of unknowns. The diagonal elements of the resulting resolution matrix denote parameter resolution whereas the off-diagonal elements denote linear dependence between the respective parameters.

In our work parameter resolution is derived as follows. If the condition number for a given source position $\theta$, $\phi$ is exceeding a value $C_{\mathrm{lim}}$, then the smallest singular value is set to zero. The $C_{\mathrm{lim}}$ depends on the overall measurement error (step quantization uncertainty, receiver noise, etc.). For a bigger measurement error, more of the smallest singular values can be set to 0 without significantly enhancing the misfit $\chi^2$ (equation (9)). Analysis shows that for the data error of 3% taken into account in this paper, $C_{\mathrm{lim}}$ is about 100. That means we can set those singular values to 0 that are inferior of 1% of the largest singular value. If so, we cancel one dimension (that which is only poorly defined by the direction-finding equations) during the solution of (14), that is, we seek a six-dimensional solution by using only five linear independent equations (five-eigenvector (EV) solution). It may seem paradoxical that the very small singular values can be zeroed, since the zeroing corresponds to skipping one linear combination of the set of equations that we are trying to solve. But we are throwing away precisely a combination of equations that is so corrupted by even small statistical errors in the observations as to be at best useless. Usually it is worse than useless since it stretches the solution vector considerably along some direction in parameter space $\mathbf{X}$ (defined by the eigenvector associated with the small singular value), and therefore may be far away from the "true solution."

In Figure 4 we show the resolution of the degree of circular polarization $V$ (Figure 4a), source colatitude $\theta$ (Figure 4b), and source azimuth $\phi$ (Figure 4c) as a function of source position given by the spherical angles $\theta$ and $\phi$ in the antenna coordinate system (Figure 2). In regions where the condition number is less than 100, the parameter resolution is unity by definition, since the number of unknowns is then equal to the number of linearly independent equations. In the other case, however, a considerable loss of parameter resolution is found. The resolution of $V$, $R(V)$ degrades as the source lies close to the Z-antenna direction. This can be understood by inspection of (7). If the source is close the Z-antenna direction, $Im < V_n V_k^* >$ tends to vanish, and the parameter $V$ is no more constrained by the direction-finding equations. Thus parameter resolution is a measure of the ability of the equation system to find a stable solution for a given parameter after finding the actual number of linear independent equations by zeroing the small and statistically insignificant singular values. The resolutions of $\theta$ ($R(\theta)$) and $\phi$ ($R(\phi)$) show a less dramatic behavior than $R(V)$; however, we note that $R(\phi)$ is degrading consider-

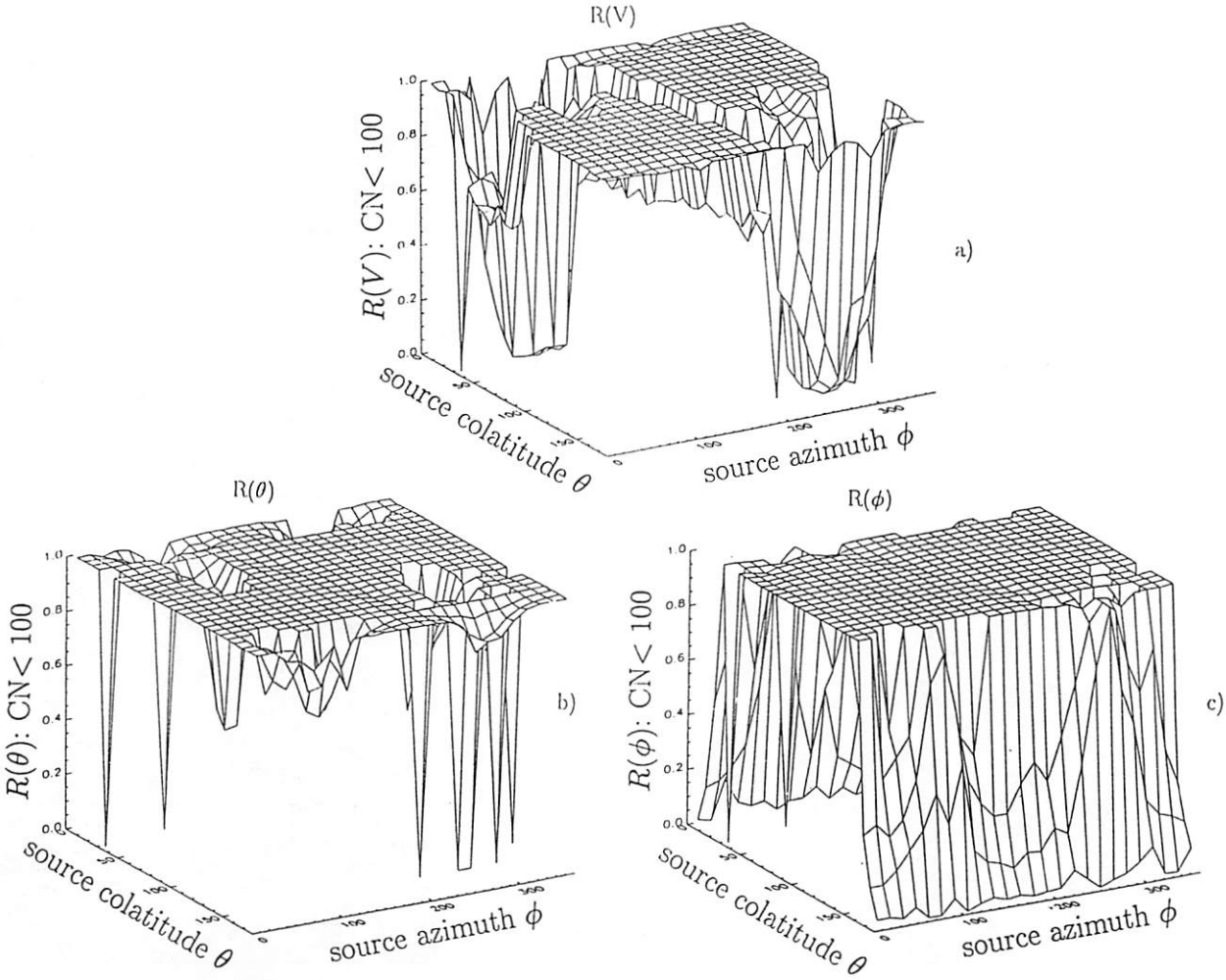


**Figure 4.** Parameter resolution of (a) $V$, (b) $\theta$, and (c) $\phi$ as a function of source antenna geometry. For antenna source geometries having a condition number larger than 100, the resolution according to the five-EV solution has been calculated.

ably when approaching the poles at $\theta = 0°$ and $\theta = 180°$ because of the geometrical dilution near the poles.

The loss of parameter resolution shown in Figure 4 is associated with growing linear dependence of parameters because we have no unique solution of the problem in parameter space. For demonstration we singled out some of the existing linear dependence of parameters in $\mathbf{X}$. In Figure 5 we show the elements of the resolution matrix ($=R_{5,1}$) corresponding to the $\theta - S$ dependence (top panel) and the $\theta - V$ dependence ($=R_{5,4}$) (bottom panel) as a function of source direction. A value of 0 means no linear dependence, and 1 or -1 is equal to perfect linear dependence. Although most regions in the $\phi$ - $\theta$ space are dominated by quasi-zero linear dependence (regions were the condition number is less than 100), there exist several regions where it is considerably distinct from 0. It is for these regions (i.e., for the associated source antenna geometry) that the concerned parameters cannot be unambiguously determined and are therefore likely to be affected by systematic errors in addition to their statistical uncertainty. For the direction-finding analyses at Saturn, the

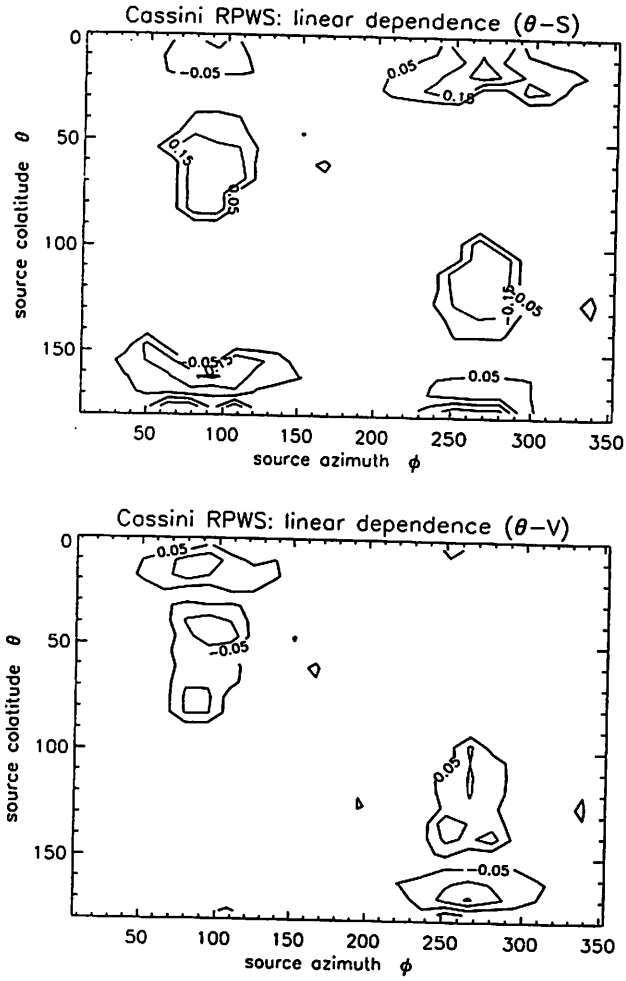


**Figure 5.** Parameter linear dependence (top) $\theta - S$ and (bottom) $\theta - V$ calculated from (15) as a function of source position for the Cassini RPWS experiment. The parameters in question do not depend on each other for a wide range of source positions; however, there exist regions where considerable linear dependence occurs, and thus no unique solution can be found for the concerned parameters.

various spacecraft-source geometries that occur when Cassini orbits around Saturn will therefore have to be checked with respect to possible linear dependencies of parameters, like in Figures 4 and 5. Similar effects, as shown in Figure 5 for the Cassini RPWS experiment, are evident for the Ulysses URAP experiment in Figure 6. The pattern is more regular for the spinning Ulysses spacecraft with negative linear dependencies for source colatitudes $\theta < 90°$ and positive ones for $\theta > 90°$. We also note that the peak values (0.2 to 0.3) are comparable for Ulysses and Cassini, however, the topography of the distributions is different, which reflects the different antenna configurations used.

A practical consequence of the occurrence of linear dependence between wave parameters is illustrated in Figure 7. The top panel shows the dependence of the source colatitude $\theta$ from the Stokes parameter $Q$ for an analyzed Jovian hectometer event ($f$=740 kHz) lasting 1 hour as observed by the Ulysses URAP experiment some 10 hours before its encounter with the planet

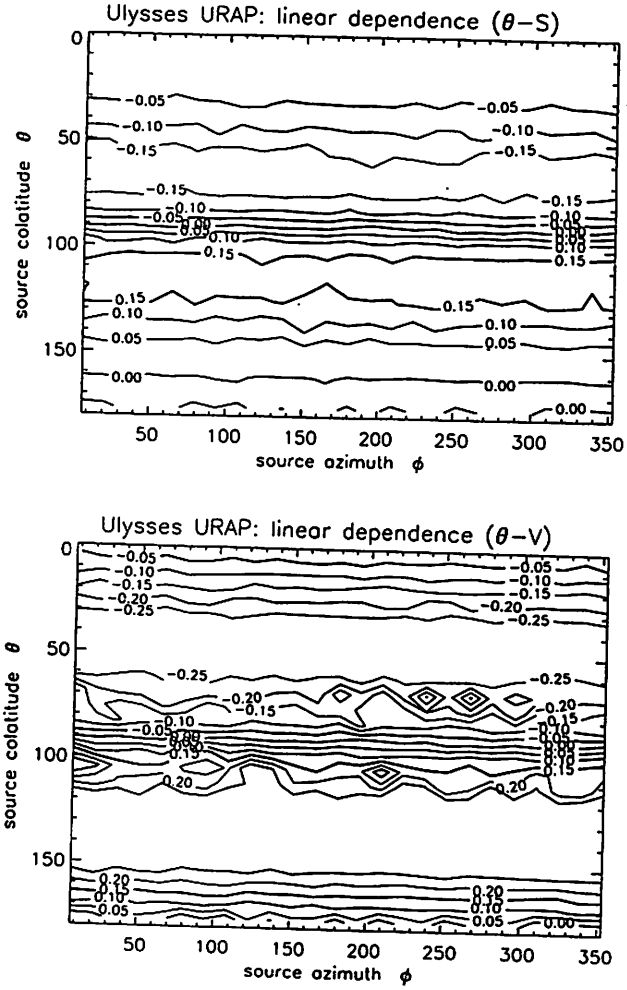


**Figure 6.** Same as Figure 5, but for the Ulysses URAP experiment.

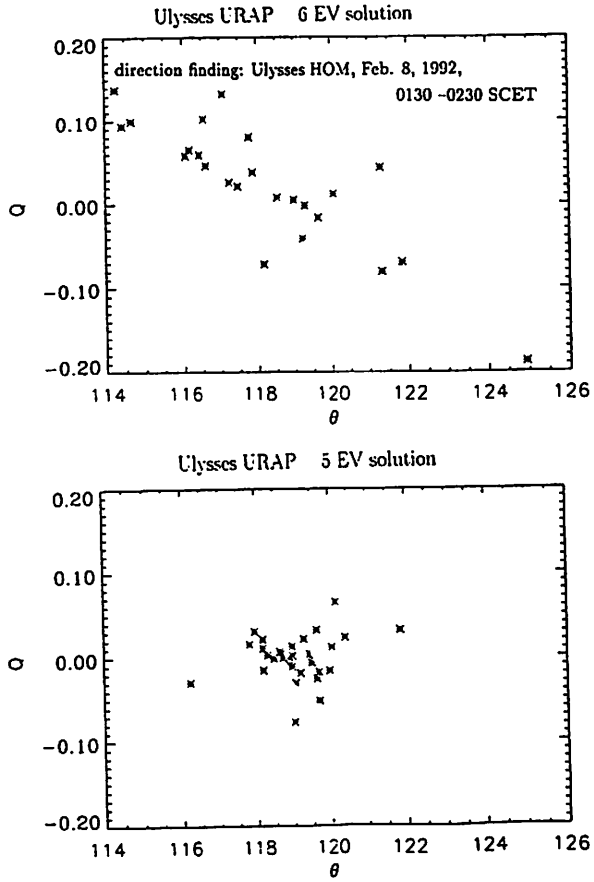


**Figure 7.** Example of linear dependence between the parameters $Q$ and $\theta$ which occurred for Ulysses URAP direction-finding results (Jovian hectometer emission (HOM) at 740 kHz observed on February 8, 1992, 0200 spacecraft event time (SCET)). (top) The parameters $Q$ and $\theta$ could not independently be determined when using the six-EV (traditional least squares fit) solution. (bottom) The five-EV solution reduced the scattering of the points and removed the linear dependence of the parameters since we added the constraint $\lambda_6 = 0$. For further discussion, see text.

Jupiter in 1992. Each plot symbol corresponds to a direction-finding solution found for an individual Ulysses spin period. The presented solution corresponds to a traditional least squares fit solution where all of the six singular values were considered for the calculation of (14) (= six-eigenvector EV solution) where the condition number was 300. Although each individual solution has been calculated independently clear linear dependence of the parameters is evident, a fact that is typical for underdetermined (ill-conditioned) systems of equations that exhibit a high condition number.

To identify those linear dependencies, we use SVD-methodologies. It may seem paradoxical that linear combinations of parameters occur for the six-EV solution where the resolution matrix is the unity matrix. However, in constructing the six-EV solution we ignored the fact that the system of direction-finding equations only has effectively five linear independent equations. In order to avoid systematically wrong solutions (due to strong amplification of measurement errors into parameter space via the very large $1/\lambda_6$ in (14)) it is imperative to cancel those combinations of equations. Zeroing $\lambda_6$ in the five-EV solution defines our (inferred) sixth equation so that no more linear dependence of parameters occurs.

For demonstration the bottom panel of Figure 7 shows the five-EV solution (the sixth (very small) singular value was zeroed) of (14) (adapted for the Ulysses URAP experiment) for the Ulysses hectometer data. The scattering of the solutions is considerably reduced and linear dependence of parameters is completely removed. The solution (in terms of source colatitude and polarization) is consequently less scattered and concentrated near $Q$=0. Indeed, the result $Q$=0 is also supported by former studies [*Reiner et al.*, 1993a, b] because it is known that the Jovian hectometric emission (HOM) does not contain any linear polarized component.

Since we have shown in Figure 5 that linear dependence between parameters will also exist for the Cassini RPWS experiment considerable improvement of the direction-finding procedure is also anticipated for the Cassini direction-finding by using singular-value decomposition analysis as described.

### 3.3. Precision of RPWS Direction Finding When Applied to the Saturnian Emissions

After the analysis of the direction-finding equations by using SVD methodologies we are now

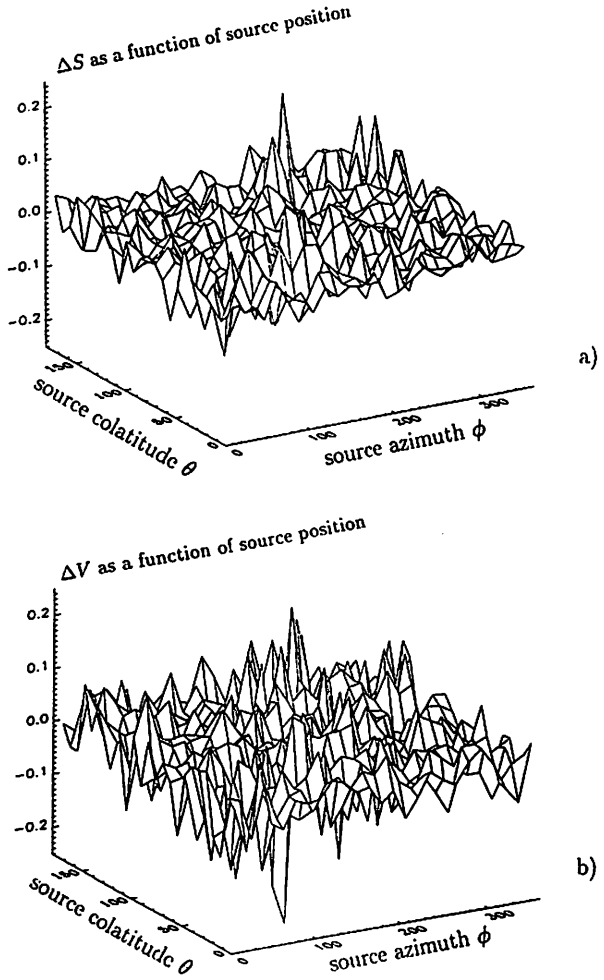


**Figure 8.** Statistical uncertainty of the 6 wave parameters (a) $\Delta S$, (b) $\Delta V$, (c) $\Delta U$, (d) $\Delta Q$, (e) $\Delta\theta$, and (f) $\Delta\phi$ as a function of source position. The statistical scattering as displayed is anticipated to be typical for the RPWS direction-finding at Saturn.

interested in what level of precision can be anticipated for the RPWS direction-finding. Simulating realistic values of $y_i^{obs}$ as discussed in section 3 we can simulate direction-finding measurements at Saturn as a function of source position. We assume that the signal to noise ratio of the received emission is high (> 20 dB), which implies a close range to Saturn for the observations, both for the precision of source localization and for this intensity requirement. Then we perform the inversion as described by (9) - (14) using the full (six-EV) solution. Thereafter, we compare the resulting wave parameters with the test wave parameters and plot the difference in Figures 8a-8f for $\Delta S$, $\Delta V$, $\Delta U$, $\Delta Q$, $\Delta\theta$, and $\Delta\phi$, respectively, as a function of source position. The scattering of points is simply due to propagation effects of the statistical error (3%) from the observations to the wave parameters throughout the inversion process, whereas the linear dependence of parameters that is anticipated for several source geometries as discussed in Figures 5 and 6 is not investigated here. The scattering in the polarization results is rather small (most of the points are within [-0.1, 0.1] concerning statistical scattering of the Stokes parameters as shown in Figures 8a-8d). As far as the scattering in source location is concerned, it is in the order of some 1°-2° in $\theta$ and $\phi$, which is sufficiently accurate to locate the SKR sources when Cassini is within, say, 10 $R_S$ from Saturn. Moreover, the error is only a statistical one which may be reduced as Cassini orbits several times around Saturn, thereby often monitoring the radio sources. Also, depending on the observing geometry and the resulting condition number of $\Lambda$, further improvement on the results is anticipated using the five-EV solution when necessary and useful as shown in Figure 7 for the Ulysses results.

## 4. Conclusion

This report includes several important aspects of the RPWS direction-finding procedure using three noncoplanar electrical antennas. Based on generalized inversion techniques that we applied to the RPWS direction-finding formalism, we show strong evidence that the direction-finding capabilities of the RPWS instrument are at least as excellent as those of the Ulysses URAP experiment, which used two synthesized, inclined spinning dipoles. Due to the fact that Cassini will orbit for several years in the vicinity of Saturn, we expect spectacular direction-finding results that will enable us to definitely understand important aspects of wave physics (e.g., generation and propagation of waves at various frequencies) in the Saturnian magnetosphere.

This paper also showed that the traditional least squares formalism is generally not sufficient to account for the complex nature of reduced parameter resolution well-known in ill-conditioned systems of equations.

The present work focuses on the direction-finding of electrically short antennas, that is, the wavelength is long compared to the dimensions of the antenna system. For higher frequencies (greater than $\approx$ 5 MHz, as, for example, SED emissions) the simple concept of a purely real effective height vector that is independent of the direction of the incoming emission must be withdrawn and replaced by a more general concept allowing the effective height to be complex and dependent on the incoming wave's direction. Some work in this respect is in preparation.

## Appendix: Singular Value Decomposition (SVD)

There exists a very powerful technique for the analysis of sets of equations which are suspected to be singular or very close to singular. In such cases where "traditional" methods like gaussian elimination or LU (lower triangular - upper triangular) decomposition fail to give satisfactory results, SVD techniques will diagnose exactly what the problem is and give possibilities for a solution. Therefore, SVD is the method of choice for solving most of linear (or linearized) least squares problems, as is the case for our direction-finding equations. SVD is based on a theorem of linear algebra which states that any $M \times M$ matrix $A$ ($M$ is the number of rows, $N$ is the number of columns), can be written as the product of an $M \times M$ column-orthogonal matrix $U$, an $N \times N$ diagonal matrix $\Lambda$ with positive, or zero elements and the transpose of an $N \times N$ orthogonal matrix $V$ [*Press et al.*, 1986]

$$A = U \Lambda V^T \tag{A1}$$

and, similarly,

$$A^T = V \Lambda U^T \tag{A2}$$

which yields

$$A^T A = V \Lambda^2 V^T \tag{A3}$$

$$A A^T = U \Lambda^2 U^T \tag{A4}$$

since $U^T U$ and $V^T V$ are equal to the identity matrix. These decompositions can always be done, no matter how singular the matrix $A$ is. The diagonal elements of $\Lambda$ denote the singular values of the matrix $A$. The number of nonzero singular values of $A$ gives the basic rank of $A$ which is always less or equal to $N$. Sometimes, however, some sigular values are very close to zero (i.e., they should be considered as to be zero).

In the case of a least squares problem, the number of equations (defined by the number of rows $M$ in matrix $A$), which is identical to the number of observations $y$, is always bigger than the number of free parameters to be fitted (equal to the number of columns $N$ in $A$). The resulting set of linear equations can be written as

$$A\mathbf{x} = \mathbf{y} \tag{A5}$$

Seeking a solution according to the method of least squares we obtain the so-called normal equations [*Press et al.*, 1986].

$$A^T A\mathbf{x} = A^T \mathbf{y} \tag{A6}$$

with the solution

$$\mathbf{x} = (A^T A)^{-1} A^T \mathbf{y} \tag{A7}$$

and, after using (A1) - (A3), we obtain after some algebra

$$\mathbf{x} = V \Lambda^{-1} U^T \mathbf{y} \tag{A8}$$

which is formally identical to (14) in the main text.

**Acknowledgments.** This work was supported by the National Programs of the Austrian Academy of Sciences.

## References

Boischot, A., Comparative studies of the "radio planets," *Planetary Radio Emissions II*, edited by H. O. Rucker, S. J. Bauer, and B. M.-Pedersen, Austrian Acad. of Sci. Press, Vienna, 1988.

Connerney, J. E. P., The magnetic field of Jupiter: A generalized inverse approach, *J. Geophys. Res.*, *86*, 7679, 1981.

Kaiser, M. L., M. D. Desch, W. S. Kurth, A. Lecacheux, F. Genova, B. M. Pedersen, and D. R. Evans, Saturn as a radio source, in *Saturn*, edited by T. Gehrels and M. S. Matthews, 378, Univ. of Arizona Press, Tucson, 1984.

Kraus, J., D., Radio Astronomy, *McGraw-Hill Book Company*, New York, 1966.

Ladreiter, H. P., P. Zarka, and A. Lecacheux, Direction finding of Jovian low-frequency radio emissions: Evidence for their auroral origin, *Planet. Space Sci.*, 11, 919, 1994.

Lecacheux, A., Direction finding of a radiosource of unknown polarization with short electric antennas on a spacecraft, *Astron. Astrophys., 70*, 701, 1978.

Manning, R., and J. Fainberg, A new method of measuring radio source parameters of a partially polarized distributed source from spacecraft observations, *Space Sci. Instrum., 5*, 161, 1980.

Press, W. H., B. P. Flannery, S. A. Teukolsky, and W. T. Vetterling, *Numerical Recipes, the Art of Scientific Computing*, Cambridge Univ. Press, New York, 1986.

Reiner, M. J., J. Fainberg, R. G. Stone, M. L. Kaiser, M. D. Desch, R. Manning, P. Zarka, and B. M. Pedersen, Source characteristics of Jovian narrow-band kilometric radio emissions, *J. Geophys. Res., 98*, 13,163, 1993a.

Reiner, M. J., J. Fainberg, and R. G. Stone, Source characteristics of Jovian hectometric radio emissions, *J. Geophys. Res., 98*, 18,767, 1993b.

Stone, R. G., and the Unified Radio and Plasma Wave science team, The unified radio and plasma wave investigation, *Astron. Astrophys. Suppl. Series, 92*, 291, 1992.

Zarka, P., Saturn electrostatic discharges: Characteristics, comparison to planetary lightning and importance in the study of Saturn's ionosphere, in *Planetary Radio Emissions*, edited by H. O. Rucker and S. J. Bauer, Austrian Acad. of Sci. Press, Vienna, 1985.

---

D. A. Gurnett and W. S. Kurth, Department of Physics and Astronomy, University of Iowa, Iowa City, IA 52242, USA. (e-mail: dag@space.physics.uiowa.edu; wsk@space.physics.uiowa.edu)

H. P. Ladreiter, W. Macher, and H. O. Rucker, Space Research Institute, Austrian Academy of Sciences, Halbaerthgasse 1, A-8010 Graz, Austria. (e-mail: hpl@bimgs1.kfunigraz.ac.at; wom@bimgs1.kfunigraz.ac.at; hor@bimgs1.kfunigraz.ac.at)

A. Lecacheux, R. Manning, and P. Zarka, Observatoire de Paris, F-92195 Meudon, Principal Cedex, France. (e-mail: mesopd::alx; meudon::manning; mesopd::zarka)

(Received January 24, 1995; revised August 11, 1995; accepted August 15, 1995.)